Poly(vinyl chloride) (PVC) Coated Idea Revisited: Influence of Carbonization Procedures on PVC-Coated Natural Graphite as Anode Materials for Lithium Ion Batteries

ARTICLE *in* THE JOURNAL OF PHYSICAL CHEMISTRY C · APRIL 2008

Impact Factor: 4.77 · DOI: 10.1021/jp8003536

4 AUTHORS, INCLUDING:

Feng Li
Chinese Academy of Sciences
213 PUBLICATIONS **14,051** CITATIONS
SEE PROFILE

Chang Liu
Nanjing University of Technology
149 PUBLICATIONS **5,686** CITATIONS
SEE PROFILE

Hui-Ming Cheng
Shenyang National Laboratory for Material…
490 PUBLICATIONS **33,789** CITATIONS
SEE PROFILE

Poly(vinyl chloride) (PVC) Coated Idea Revisited: Influence of Carbonization Procedures on PVC-Coated Natural Graphite as Anode Materials for Lithium Ion Batteries

Hong-Li Zhang, Feng Li, Chang Liu, and Hui-Ming Cheng*

Shenyang National Laboratory for Materials Science, Institute of Metal Research, Chinese Academy of Sciences, 72 Wenhua Road, Shenyang 110016, China

Received: January 14, 2008; Revised Manuscript Received: March 9, 2008

The influence of carbonization procedures on poly(vinyl chloride) (PVC) coated natural graphite (NG) spheres as anode materials for lithium ion batteries was investigated in detail in this study. At first, thermogravimetry−mass spectrometry was utilized to analyze pyrolysis behaviors of PVC, and on the basis of the results three typical carbonization procedures consisting of different heating steps were determined to fabricate PVC-coated NG spheres. The structural parameters, morphologies, pore size distributions, and Brunauer–Emmett–Teller specific surface areas of these coated samples were systematically characterized by employing X-ray diffraction, Raman spectroscopy, scanning electron microscopy, and N_2 adsorption/desorption isotherms. Electrochemical performance measurements indicated that all the coated samples display a significantly improved cyclability, rate capability, and initial Coulombic efficiency in comparison with the pristine NG spheres. The reasons for the performance improvement were further explored using electrochemical impedance spectroscopy. Moreover, the sample under the carbonization procedure involving isothermal heating steps at temperatures of 280, 450, and 900 °C is even better than the well-recognized mesocarbon microbeads in terms of reversible capacity and rate capability.

1. Introduction

Since the birth of commercial lithium ion batteries (LIB) in the early 1990s, various kinds of carbonaceous materials including graphitic and nongraphitic carbons, tin oxides and alloys, Si-based composites, etc. have been extensively investigated as anode materials.[1–5] However, only graphitic carbon, especially synthetic graphite, is dominantly used in practical applications due to its high reversibility and flat voltage profile during Li^+ intercalation/deintercalation.[6,7] Nevertheless, the relatively high cost of synthetic graphite such as mesocarbon microbeads (MCMB) is an impediment to producing inexpensive LIB.[8] From an economic point of view, natural graphite (NG) with intrinsically high crystallinity is attractive and competitive as an anode material to replace synthetic graphite, because it is an abundant resource and is low cost.[9,10] Unfortunately, the large irreversible capacity loss, poor cyclability and rate capability of NG limit its direct use in LIB.[11] So far, a lot of modification methods for NG have been attempted: (i) constructing a core–shell structure by coating NG with nongraphitic carbon [12–19] and metals such as Ag, Cu, Ni, etc.;[20,21] (ii) changing the surface chemical or physical state of NG by gas mild oxidation,[22,23] liquid oxidant treatment,[24,25] mechanical milling,[26,27] etc.

Poly(vinyl chloride) (PVC) is one of the most common polymers with low price and large production amount each year.[28] In this study, we revisit a PVC-coated idea to modify a kind of NG spheres, whose capacity fading mechanisms have been explored by us.[29] In fact, the PVC-coated idea has been extensively adopted by others to prepare carbon-coated ceramic,[30] transition metal,[31] and graphite [32–34] particles, etc. However, these works all utilized a conventional continuous heating way, i.e. directly heating to a terminal temperature without any intermediate tarries, to carbonize PVC. Generally, they cannot always guarantee a proper coverage and adherence of PVC-carbonized products on the particle surfaces. Herein, we propose a new strategy, adding multiple heating steps in a carbonization procedure, to easily achieve a good coating effect of PVC. First, on the basis of pyrolysis behaviors of PVC from thermogravimetry−mass spectrometry (TG−MS), we determined three typical carbonization procedures consisting of different heating steps to fabricate PVC-coated NG spheres. Then, the changes and differences in structure, morphology, specific surface area, pore size distribution, and hydrogen (H) content were systematically studied among the pristine and coated samples. Finally, we investigated the electrochemical performance of all the coated samples as LIB anode materials: their cyclability, rate capability, and initial Coulombic efficiency (CE) are significantly improved relative to the pristine NG. The reasons for the performance improvement were further analyzed according to the results of electrochemical impedance spectroscopy (EIS). In addition, we also demonstrated that the sample under a particular carbonization procedure is also better than commercial MCMB in terms of reversible capacity and rate capability.

2. Experimental Section

2.1. Sample Preparation and Characterization. NG spheres (average size ~20 μm, from Qingdao, China) and PVC powders (average polymerization degree of ~1000, from Jinhua Chemical Group, China) were used as received commercially. First, NG (1 g) was added into the solution containing PVC (1.4 g) and 1,2-epoxypropane (60 mL). After immersion for 30 min under ultrasonic stirring, the solution was then evaporated. In this way, PVC could sufficiently enter the surface cracks of NG. Meanwhile, PVC also existed on the surface with no cracks. Subsequently, the immersed samples were subjected to three different carbonization procedures in a tube furnace in Ar

* Corresponding author. Fax: +86 24 2390 3126. E-mail: cheng@imr.ac.cn.

10.1021/jp8003536 CCC: $40.75
Published on Web 04/29/2008

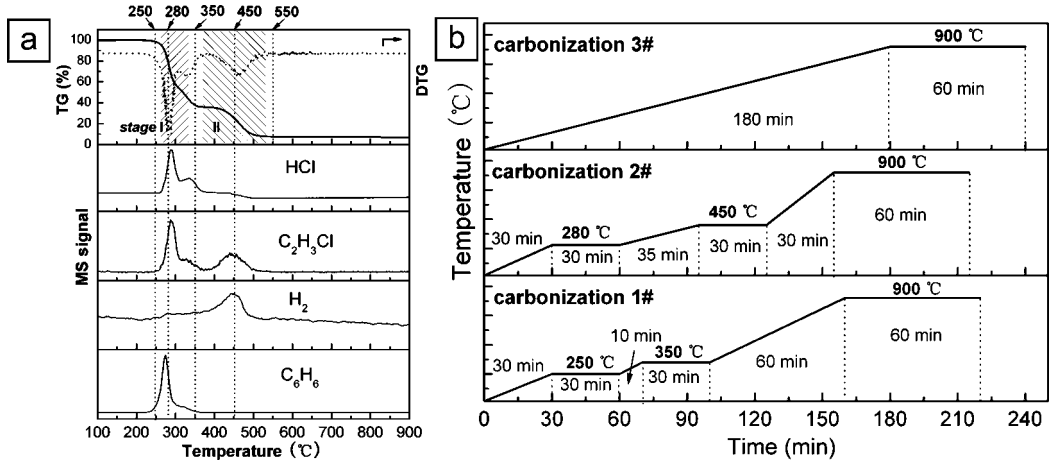

Figure 1. (a) TG−MS data of PVC. (b) Diagram showing the detailed multistep heating in the three carbonization procedures.

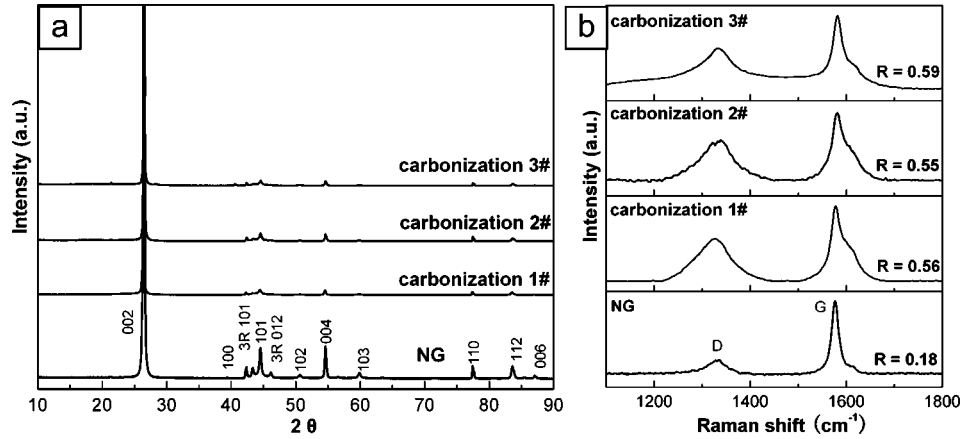

Figure 2. (a) XRD patterns of pristine NG and coated samples under different carbonization procedures no. 1, no. 2, and no. 3. (b) Comparison of Raman spectra for pristine and coated NG spheres.

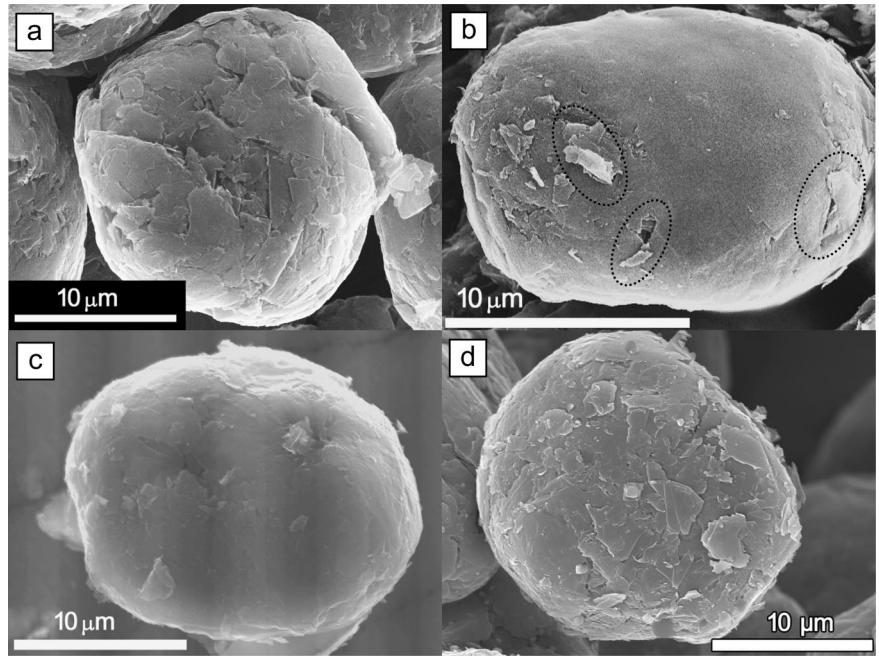

Figure 3. SEM images of pristine NG (a) and coated samples under carbonizations no. 1 (b), no. 2 (c), and no. 3 (d).

atmosphere (flow rate 100 mL/min). These carbonization procedures denoted as carbonization no. 1, carbonization no. 2, and carbonization no. 3 (illustrated in Figure 1) were established according to pyrolysis behaviors of PVC with the aid of TG−MS (Netzsch, STA 449C and QMS 403C). In order to verify the experimental reproducibility, each carbonization procedure was employed three times to fabricate three batches of PVC-coated NG spheres, and the as-obtained nine (3 × 3)

coated samples were all subject to various characterizations and measurements. The experimental results indicated good reproducibility (the error of electrochemical data was less than 1%), and the following various data we show here are representative of all results.

Scanning electron microscopy (SEM; JSM-6301F) was used to observe the morphology of the pristine and coated NG spheres. X-ray diffraction (XRD; D/max 2400 with Cu Kα radiation) and laser Raman spectroscopy (Labram HR 800, Jobin-Yvon) were utilized to characterize their structural parameters. Brunauer–Emmett–Teller (BET) specific surface area and pore size distribution (calculated using the Barrett–Joyner–Halenda method) of the pristine and coated samples were obtained from the analysis of N_2 adsorption/desorption isotherms (ASAP 2010, Micromeritics). The content of PVC-carbonized products in the coated samples was determined by two methods: one was based on TG analysis as used by Wang et al.;[35] the other was to calculate the mass increment before and after reaction. The results obtained from both methods correspond well with each other.

2.2. Electrochemical Measurements. Half-cells were assembled in an Ar-filled glovebox (Unilab, H_2O and $O_2 < 1$ ppm) with a working electrode, a lithium foil counter electrode, and a porous separator (Celgard 2400). The working electrode was prepared by coating a slurry of active material (85 wt %), carbon black (5 wt %), and poly(vinylidene fluoride) binder (10 wt %) dissolved in *N*-methylpyrrolidine onto a copper foil, and then drying in vacuum at 120 °C for 12 h. Afterward, it was cut into sheets with an area of 0.64 cm^2, and the sheets were pressed under a pressure of 3 MPa. The electrolyte was 1 M $LiPF_6$ in a mixture of ethylene carbonate and dimethyl carbonate (1:1 by volume). The cells were galvanostatically charged/discharged at different capacitance (C) rates between 0.001 and 2.5 V versus Li^+/Li. Impedance spectra were potentiostatically measured (Solartron 1260/1287) by applying an ac voltage of 5 mV amplitude over the frequency range of 100 kHz−10 mHz after electrodes had attained equilibrium at certain electrochemical states.

3. Results and Discussion

3.1. Pyrolysis Behaviors of PVC. In order to investigate pyrolysis behaviors of PVC, we performed TG−MS analysis (heating rate 10 K/min, in Ar) as shown in Figure 1a. From the TG and derivative (DTG) curves, it can be seen that there are two main stages (I and II) responsible for the weight loss in the thermal decomposition of PVC: the first stage from 250 to 350 °C and the second stage between 350 and 550 °C. Referring to the MS data below the TG−DTG curves, we can identify some typical volatile species in each stage. In stage I, HCl, C_2H_3Cl, and C_6H_6 are vigorously released, possibly due to the transformation of PVC to conjugated double-bond polyene chains. The transformation is accompanied by the elimination of chlorine-containing species (e.g., HCl, C_2H_3Cl) and the formation of some aromatic hydrocarbons (e.g., C_6H_6, $C_{10}H_8$).[36,37] In stage II, H_2 is the major volatile component with a small amount of C_2H_3Cl, which should be ascribed to the scission and condensation of polyene sequences into a three-dimensional backbone network and the aromatization of some small molecules.[38] Considering the complex pyrolysis behaviors of PVC (with many competitive and consecutive reactions), we perceive that controlling carbonization procedures, e.g., properly varying heating rates and adding intermediate isothermal steps, would affect the release of volatile compounds and the occurrence of some secondary condensation and aromatization reactions in each stage. Then, the structure and texture of PVC-carbonized products, which influence the final coating effect of PVC, can be adjusted to a certain extent.

In view of the above TG−MS results, we determine three carbonization procedures (see Figure 1b) for PVC coating: no. 1, adopting two isothermal heating steps at the starting temperatures of stages I and II (i.e., 250 and 350 °C, respectively), and the heating rates are ∼10 °C/min both from 250 to 350 °C and from 350 to 900 °C; no. 2, choosing the maximal peak temperatures of the DTG curve (i.e., 280 and 450 °C) as the constant-temperature points, and the heating rates are ∼5 °C/min between 280 and 450 and 15 °C/min between 450 and 900 °C. The determination of these heating rates is based two factors: on one hand, they should associate with the choosing of isothermal heating steps; on the other hand, the consideration of time duration is also necessary, since a carbonization procedure with a very long processing time is not attractive from an economic standpoint. For comparison, we also select the conventional carbonization procedure, no. 3, using a continuous heating to 900 °C without intermediate tarries. To improve the quality of PVC-carbonized products, the three carbonization procedures all involve an isothermal heating step at 900 °C for 1 h, as shown in Figure 1b, where the detailed heating times and rates in each carbonization procedure are given as well.

3.2. XRD and Raman Analysis. Figure 2a presents the XRD patterns of the pristine and coated NG spheres. It can be seen that all the coated samples have a 002 diffraction peak (position and symmetry) similar to that of the pristine NG, indicating that their overall structural characteristics are not severely changed after coating. This is chiefly due to a small weight percentage of PVC-carbonized products in these coated samples: 15.4%, 14.1%, and 13.2% corresponding to carbonizations no. 1, no. 2, and no. 3, respectively. Based on these values along with the diameter of pristine NG spheres (∼20 μm) and the related carbon densities (NG, ∼2.2 g/cm^3; PVC-carbonized product, ∼1.7 g/cm^3), we can further estimate the thickness of each carbon layer derived from PVC as approximately 780, 700, and 650 nm. Comparison of their Raman spectra is displayed in Figure 2b, where the pristine NG exhibits a distinct G-band and a weak D-band with a low intensity ratio of I_D/I_G (0.18, defined as *R* value), a typical feature of highly crystallized graphite. On the contrary, the spectra of the coated samples become widening and have larger *R* values (no. 1, 0.56; no. 2, 0.55; no. 3, 0.59), which evidently reveals the existence of the thin PVC-carbonized layer on the surface and the contribution of its nongraphitic structure. From the similar *R* values among the coated samples, it can be concluded that the three different carbonization procedures exert almost the same influence on the quality (crystallinity or graphitization degree) of the PVC-carbonized products.

3.3. Morphological Characteristics of the Pristine and Coated NG. Figure 3 shows SEM images of pristine and coated NG spheres. It can be observed that there are many cracks on the surface of pristine NG (see Figure 3a). During electrochemical cycling, electrolytes can easily penetrate the inside of NG spheres through these cracks, and decompose there with the formation of internal solid electrolyte interphase (SEI) film and the production of gases (e.g., C_2H_4) that cause the expansion of NG spheres and the exfoliation of surface graphite flakes.[29] As a result, a poor cyclability is unavoidable for the pristine NG as LIB anode material.

For the coated sample under carbonization no. 1, most of its surface is smoothly covered by PVC-carbonized products as shown in Figure 3b. However, the coverage is not coherent and

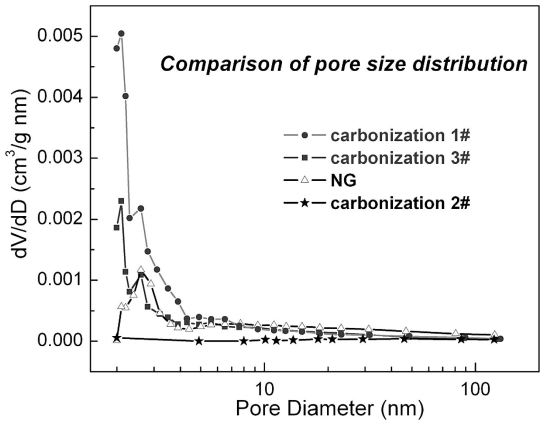

Figure 4. Comparison of pore size distribution for pristine NG and coated samples under different carbonization procedures.

TABLE 1: Summary of BET Specific Surface Area, H Content, and Electrochemical Capacity for Pristine and Coated NG

			electrochemical capacity (mA·h/g)	
sample	BET area (m^2/g)	H content (wt %)	first cycle	30th cycle
NG	4.3	0.055	314	163
carbonization no. 1	36	0.24	378	284
carbonization no. 2	1.4	0.14	330	334
carbonization no. 3	5.5	0.16	345	250

compact with the existence of some fragments, holes, and splits on the surface (marked by ellipses), which cannot effectively inhibit the penetration of electrolytes and will deteriorate electrochemical cyclic performance of the sample in the long run. In contrast, for the sample under carbonization no. 2, the cracks are closely and firmly united by the PVC-carbonized products as fillers (see Figure 3c). The coverage and filling, we believe, should bring a significant improvement in electrochemical performance (e.g., cyclability). The sample under carbonization no. 3 is presented in Figure 3d, where the PVC-carbonized products exist as many loose fragments that may gradually detach from the NG spheres owing to the immersion and peeling of electrolytes. The obvious differences in coating morphology among these coated samples sufficiently prove the importance of selection of a proper carbonization procedure when using PVC as a coating precursor. Herein, carbonization no. 2, including the unique intermediate heating steps at the peak temperatures of the DTG curve, sets a good example for the achievement of an almost perfect coating.

3.4. Pore Size Distribution and BET Specific Surface Area. To further compare the coating effects of different carbonization procedures, we carried out the analyses of pore size distribution as shown in Figure 4. The pristine NG and the coated samples under carbonizations no. 1 and no. 3 mainly display the presence of pores in the range 2−5 nm. However, the sample of carbonization no. 2 shows almost no changes in the curve of the pore size distribution under the current scale of vertical coordinate, which indicates that the PVC-carbonized products nearly fill all surface cracks on the NG spheres, in agreement with the morphological observation in Figure 3c. On the other hand, it is quantitatively learnt that the cumulative pore volume of the no. 2 sample is reduced to 0.0054 from 0.025 cm^3/g of the pristine NG. In addition, the BET surface area also shows a remarkable decrease from 4.3 to 1.4 m^2/g as given in Table 1. Generally, a low BET area will be beneficial for a high initial CE of electrode materials in LIB. There are two factors influencing the BET areas of coated samples: the texture of PVC-carbonized products themselves and their coherent effect with NG spheres. Under the carbonization procedures of no. 1 and no. 3, an insufficient releasing of some volatile species (HCl, C_2H_3Cl, C_6H_6, etc.) may cause some mesopores in the texture of PVC-carbonized products. Meanwhile, the coherent effect of no. 1 and no. 3 samples is not good enough (as shown in Figure 3b,d). Therefore, the BET areas of the no. 1 (36 m^2/g) and no. 3 (5.5 m^2/g) samples are yet increased in comparison with that of pristine NG. In a word, the variations in specific surface area and pore size distribution for the coated samples again confirm the crucial role of an appropriate carbonization procedure in achieving a good coating effect of PVC.

3.5. Electrochemical Properties. Figure 5 displays the comparison of electrochemical performance for pristine NG and coated samples. It can be seen that the capacity of pristine NG fades rapidly with the increase of cycle numbers, especially in the initial stages. However, the coated samples all demonstrate an improved cyclability and rate capability (at different C-rates ranging from 0.1 to 1.2 C, as given in Figure 5b), and the first CE is also raised from 80% for pristine NG to 83%, 87%, and 82% for no. 1, no. 2, and no. 3 samples, respectively. Moreover, the irreversible capacity loss of each sample at the first cycle, which is related to the formation of SEI film and the trapping of Li^+ in certain active sites of electrode materials, is as follows: pristine NG, 78 mA·h/g; no. 1 sample, 77 mA·h/g; no. 2 sample, 49 mAh/g; no. 3 sample, 75 mA·h/g. With regard to the performance differences among the coated samples themselves, it is exactly what we have anticipated in comparing their morphological characteristics that the no. 2 sample should be superior because of its good coating effect. In Table 1, we contrast the initial capacity and the capacity at the 30th cycle for different anode materials. It can be noted that excellent capacity retention is achieved by the no. 2 sample, although its initial capacity is lower than those of the other two coated samples. We compared the H content in each sample (see Table 1) and found that the sample containing a high H content has a large initial electrochemical capacity, which is consistent with what Zheng et al.[39] reported about the relationship between the H content and the capacity of carbonaceous materials. Furthermore, the high H contents in no. 1 and no. 3 samples indirectly verify our above speculation that insufficient release of some volatile species (e.g., HCl, C_2H_3Cl, and C_6H_6) occurs in the carbonization procedures of no. 1 and no. 3.

To investigate the reasons for the remarkable performance improvement between pristine NG and the no. 2 sample more deeply, EIS was employed as a powerful tool to characterize their impedance changes. (In our EIS testing, we tried to make the geometric factors of electrodes, which can influence the EIS spectra as well,[40] be similar for the two samples.) Figure 6 exhibits Nyquist plots of the two samples at different electrochemical states: one was freshly kept at open-circuit voltage (OCV), and the other was first discharged to 0.1 V. In Figure 6a, both samples show typical behavior of a blocking electrode with a straight line rising at an angle of ~90° to the Z'-axis. As for the semicircles in the zoom part (see inset of Figure 6a), they reflect the intrinsic electronic resistance of electrodes and the contact resistance of interparticles of electroactive materials.[41] It can be seen that the semicircle for the no. 2 sample is smaller than that for pristine NG, and so is the related resistances. This low electrode resistance is helpful for the no. 2 sample to decrease electrode polarization and maintain

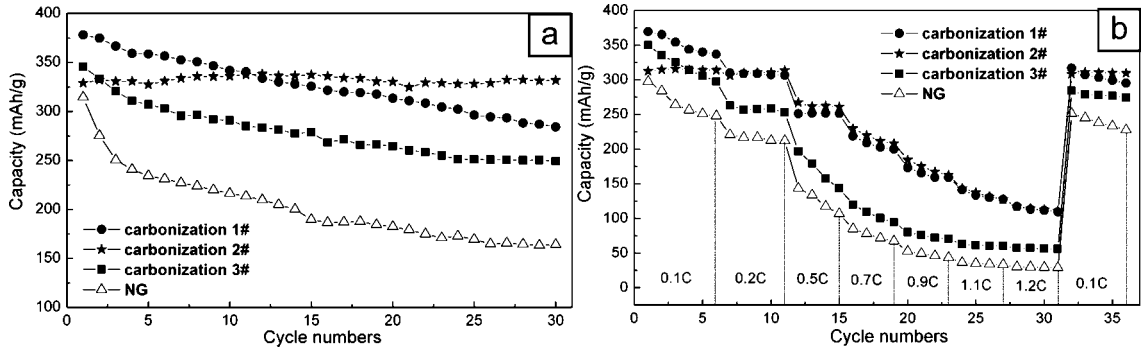

Figure 5. Comparison of electrochemical performance for pristine NG and coated samples: (a) cyclability at 0.1 C; (b) rate capability at different C-rates.

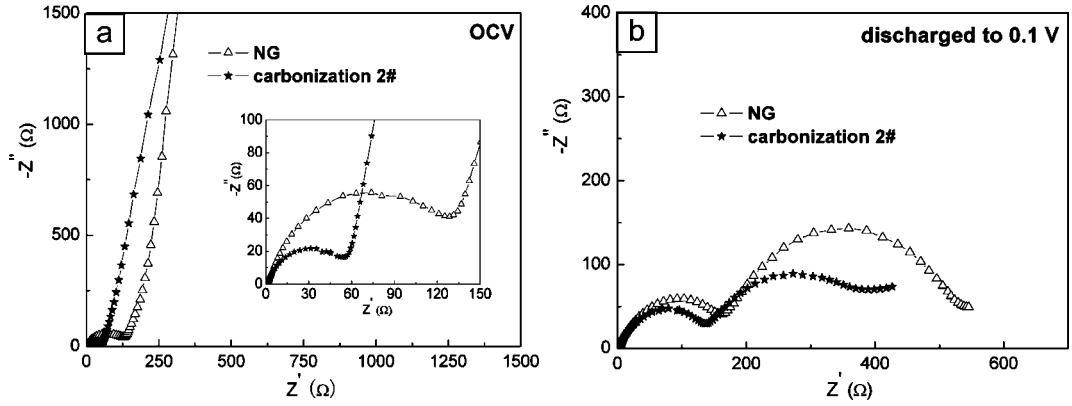

Figure 6. Comparison of Nyquist plots obtained at OCV (a) and 0.1 V (b) for the pristine NG and no. 2 sample. Inset in (a) is the zoom part of high-to-medium frequency.

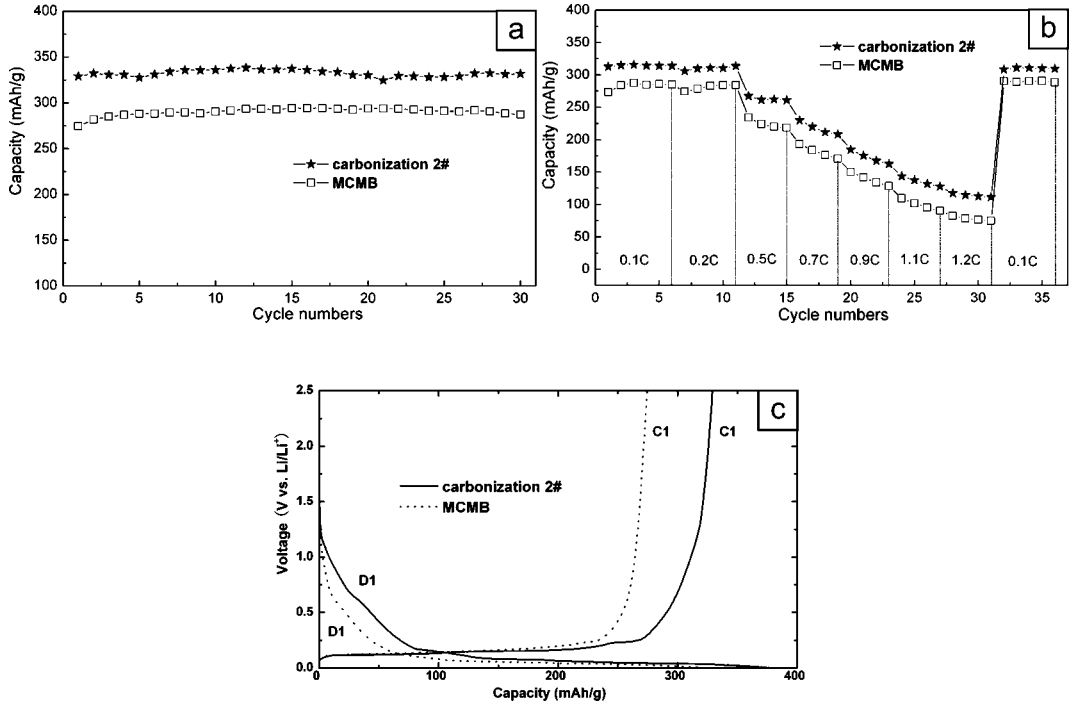

Figure 7. Comparison of electrochemical properties for no. 2 sample and a commercial MCMB: (a) cyclability at 0.1 C; (b) rate capability at different C-rates; (c) voltage profiles for the first discharge (denoted as D1) and charge (C1) processes.

stable electrochemical states at high C-rates. In Figure 6b, the Nyquist plot shows two depressed semicircles, where the first one in the high-frequency region generally corresponds to the impedance of SEI film and the second one in the medium-to-low frequency region correlates with the impedance of charge transfer.[42,43] It can be clearly noted that the impedances of both SEI film and charge transfer for the no. 2 sample are lowered in comparison with those of pristine NG, which again reveals the advantages and functions of the nongraphitic PVC-carbonized layer from the electrochemical standpoint. Further studies on the variations of EIS spectra after different cycle numbers are in progress.

In Figure 7a,b, the electrochemical properties of the no. 2 sample are compared with those of the most recognized MCMB (heat treatment at 2800 °C, Osaka Gas Co., Ltd.), which is commonly utilized as an evaluating reference.[44,45] It is exciting to note that the no. 2 sample is better than the commercial MCMB in terms of reversible capacity and rate capability. Figure 7c presents voltage profiles of the two samples during the first discharge/charge process. It can be seen that the merits of NG, a low voltage plateau and small voltage hysteresis, are well preserved in the no. 2 sample. Meanwhile, no obvious plateaus at ~0.75 V, generally corresponding to the intense formation of SEI film and the large loss of irreversible capacity,[46] are found for the no. 2 sample due to its proper coating effect (with a low specific surface area of 1.4 m^2/g). Consequently, the no. 2 sample, obtained using the simple modification method of carbonization no. 2, is promising for the practical application in commercial LIB.

4. Conclusions

On the basis of pyrolysis behaviors of PVC from TG−MS, three typical carbonization procedures were determined for the fabrication of PVC-coated NG spheres. The influence of these carbonization procedures on the structural parameters of the coated samples is negligible, but the influence on morphologies, specific surface areas, pore size distributions, and electrochemical performance are significant. Under the condition of carbonization no. 2 that specially employs two intermediate isothermal heating steps at 280 and 450 °C, the no. 2 sample morphologically exhibits a very compact and firm coating feature, and the pore volume and BET surface area of the sample are also notably decreased to 0.0054 cm^3/g and 1.4 m^2/g, respectively. Electrochemical performance measurements indicate that a reversible capacity of above 330 mA·h/g can be maintained with stable cyclability for the no. 2 sample, which is not only better than pristine NG but also a commercial MCMB. The reasons for the performance improvement are mainly ascribed to the proper coating effect and the lowered impedances of SEI film and charge transfer.

Moreover, the way here to determine a proper carbonization procedure for PVC using TG−MS, we believe, is also revelatory for those who are utilizing other polymers (e.g., polyethylene, poly(vinyl alcohol), propylene, polystyrene) as precursors to fabricate carbon-coated ceramic, transition metal, and oxide materials. We strongly recommend that multistep heating in a carbonization procedure should be seriously considered in order to achieve an excellent coating effect and thus superior physicochemical properties of carbon-coated materials.

Acknowledgment. The work was supported by the National Natural Science Foundation of China (Nos. 90606008, 50632040, and 50472084), and the Chinese Academy of Sciences.

References and Notes

(1) Tarascon, J. M.; Armand, M. *Nature* **2001**, *414*, 359.
(2) Kida, Y.; Yanagida, K.; Funahashi, A.; Nohma, T.; Yonezu, I. *J. Power Sources* **2001**, *94*, 74.
(3) Wakihara, M. *Mater. Sci. Eng., R* **2001**, *33*, 109.
(4) Tirado, J. L. *Mater. Sci. Eng., R* **2003**, *40*, 103.
(5) Kasavajjula, U.; Wang, C. S.; Appleby, A. J. *J. Power Sources* **2007**, *163*, 1003.
(6) Wu, Y. P.; Rahm, E.; Holze, R. *J. Power Sources* **2003**, *114*, 228.
(7) Cao, F.; Barsukov, I. V.; Bang, H. J.; Zaleski, P.; Prakash, J. *J. Electrochem. Soc.* **2000**, *147*, 3579.
(8) Shim, J.; Striebel, K. A. *J. Power Sources* **2007**, *164*, 862.
(9) Herstedt, M.; Fransson, L.; Edström, K. *J. Power Sources* **2003**, *124*, 191.
(10) Zaghib, K.; Song, X.; Guerfi, A.; Rioux, R.; Kinoshita, K. *J. Power Sources* **2003**, *119–121*, 8.
(11) Zhang, W. H.; Fang, L.; Yue, M.; Yu, Z. L. *J. Power Sources* **2007**, *174*, 766.
(12) Zhang, H. L.; Liu, S. H.; Li, F.; Bai, S.; Liu, C.; Tan, J.; Cheng, H. M. *Carbon* **2006**, *44*, 2212.
(13) Yoshio, M.; Wang, H. Y.; Fukuda, K.; Hara, Y.; Adachi, Y. *J. Electrochem. Soc.* **2000**, *147*, 1245.
(14) Natarajan, C.; Fujimoto, H.; Tokumitsu, K.; Mabuchi, A.; Kasuh, T. *Carbon* **2001**, *39*, 1409.
(15) Wang, H. Y.; Yoshio, M. *J. Power Sources* **2001**, *93*, 123.
(16) Wang, G. P.; Zhang, B.; Yue, M.; Xu, X. L.; Qu, M. Z.; Yu, Z. L. *Solid State Ionics* **2005**, *176*, 905.
(17) Han, Y. S.; Lee, J. Y. *Electrochim. Acta* **2003**, *48*, 1073.
(18) Zhou, Y. F.; Xie, S.; Chen, C. H. *Electrochim. Acta* **2005**, *50*, 4728.
(19) Ding, Y. S.; Li, W. N.; Iaconetti, S.; Shen, X. F.; Dicarlo, J.; Galasso, F. S.; Suib, S. L. *Surf. Coat. Technol.* **2006**, *200*, 3041.
(20) Choi, W. C.; Byun, D. J.; Lee, J. K.; Cho, B. W. *Electrochim. Acta* **2004**, *50*, 523.
(21) Takamura, T. *Bull. Chem. Soc. Jpn.* **2002**, *75*, 21.
(22) Peled, E.; Menachem, C.; Bar-Tow, D.; Melman, A. *J. Electrochem. Soc.* **1996**, *143*, L4.
(23) Menachem, C.; Wang, Y.; Floners, J.; Peled, E.; Greenbaum, S. G. *J. Power Sources* **1998**, *76*, 180.
(24) Wu, Y. P.; Jiang, C.; Wan, C.; Holze, R. *J. Power Sources* **2002**, *111*, 329.
(25) Ein-Eli, Y.; Koch, V. R. *J. Electrochem. Soc.* **1997**, *144*, 2968.
(26) Natarajan, C.; Fujimoto, H.; Mabuchi, A.; Tokumitsu, K.; Kasuh, T. *J. Power Sources* **2001**, *92*, 187.
(27) Wang, H. Y.; Ikeda, T.; Fukuda, K.; Yoshio, M. *J. Power Sources* **1999**, *83*, 141.
(28) Qiao, W. M.; Song, Y.; Yoon, S. H.; Korai, Y.; Mochida, I.; Yoshiga, S.; Fukuda, H.; Yamazaki, A. *Waste Manage.* **2006**, *26*, 592.
(29) Zhang, H. L.; Li, F.; Liu, C.; Tan, J.; Cheng, H. M. *J. Phys. Chem. B* **2005**, *47*, 22205.
(30) Inagaki, M.; Miura, H.; Konno, H. *J. Eur. Ceram. Soc.* **1998**, *18*, 1011.
(31) Inagaki, M.; Okada, Y.; Miura, H.; Konno, H. *Carbon* **1999**, *37*, 329.
(32) Tsumura, T.; Katanosaka, A.; Souma, I.; Ono, T.; Aihara, Y.; Kuratomi, J.; Inagaki, M. *Solid State Ionics* **2000**, *135*, 209.
(33) Lee, H. Y.; Baek, J. K.; Jang, S. W.; Lee, S. M.; Hong, S. T.; Lee, K. Y.; Kim, M. H.; et al. *J. Power Sources* **2001**, *101*, 206.
(34) Imanishi, N.; Ono, Y.; Hanai, K.; Uchiyama, R.; Liu, Y.; Hirano, A.; Takeda, Y.; Yamamoto, O. *J. Power Sources*, in press, http://dx.doi.org/10.1016/j.jpowsour.2007.09.035.
(35) Wang, H. Y.; Yoshio, M.; Abe, T.; Ogumi, Z. *J. Electrochem. Soc.* **2002**, *149*, A499.
(36) Marcilla, A.; Beltran, M. *Polym. Degrad. Stab.* **1996**, *53*, 251.
(37) Qiao, W. M.; Yoon, S. H.; Korai, Y.; Mochida, I.; Inoue, S.; Sakurai, T.; Shimohara, T. *Carbon* **2004**, *42*, 1327.
(38) Miranda, R.; Yang, J.; Roy, C.; Vasile, C. *Polym. Degrad. Stab.* **1999**, *64*, 127.
(39) Zheng, T.; Liu, Y. H.; Fuller, E. W.; Tseng, S.; Sacken, U.; Dahn, J. R. *J. Electrochem. Soc.* **1995**, *142*, 2581.
(40) Mantia, F. L.; Vetter, J.; Novák, P. *Electrochim. Acta*, in press, http://dx.doi.org/10.1016/j.electacta.2007.12.060.
(41) Song, J. Y.; Lee, H. H.; Wang, Y. Y.; Wan, C. C. *J. Power Sources* **2002**, *111*, 255.
(42) Funabiki, A.; Inaba, M.; Ogumi, Z.; Yuasa, S. I.; Otsuji, J.; Tasaka, A. *J. Electrochem. Soc.* **1998**, *145*, 172.
(43) Aurbach, D. *J. Power Sources* **2000**, *89*, 206.
(44) Yoshio, M.; Wang, H. Y.; Fukuda, K.; Umeno, T.; Abe, T.; Ogumi, Z. *J. Mater. Sci.* **2004**, *14*, 1754.
(45) Barsukov, I. V.; Henry, F. B.; Doninger, J. E.; Zaleski, P. L.; Gallego, M. A.; Huerta, T.; Uribe, G.; Girkant, R.; Derwin, D. *ITE Battery Lett.* **2003**, *4*, 163.
(46) Yazami, R.; Deschamps, M.; Genies, S.; Frison, J. C. *J. Power Sources* **1997**, *68*, 110.

JP8003536